Title: Agile allocation in the tundra: a single growing season of warming increases nutrient availability while decreasing fine root length

Running Title: Rapid tundra response

Authors: Verity G. Salmon[1*], Alistair Rogers[2,3], Joanne Childs[1†], Kim S. Ely[2,3], Shawn Serbin[4], Breann Spencer[5], Keith Lewin[3ϕ], Richard J. Norby [1,6], Colleen M. Iversen[1]

Affiliations:

[1]Environmental Sciences Division, Oak Ridge National Laboratory, Oak Ridge, TN, USA
[2]Climate and Ecosystem Sciences Division, Lawrence Berkeley National Laboratory, Berkeley, CA, USA
[3]Environmental and Climate Sciences Department, Brookhaven National Laboratory, Upton, NY, USA
[4] Biospheric Sciences Laboratory, NASA Goddard Space Flight Center, Greenbelt, MD
[5]Savanna River Ecology Laboratory, University of Georgia, Aiken, SC
[6] Department of Ecology and Evolutionary Biology, University of Tennessee, Knoxville, TN, USA

[*] corresponding author
[†] deceased
[ϕ] retired

Corresponding author: Verity G. Salmon (salmonvg@ornl.gov; 925-878-9681)

Author Contributions: VGS, AR, SS, RJN, & CMI participated in securing funding and planning this research. AR, KSE, & KL were integral to design and deployment of Zero Power Warming chambers. VGS, AR, JC, KSE, SS, BS, & CMI collected data. Lab work was performed by VGS, JC, KSE, & BS. Data analysis was done by VGS, KSE, SS, & BS. VGS wrote the initial draft of the manuscript and AR, JC, KSE, SS, BS, RJN, and CMI provided feedback integral to the final version of the paper.

Keywords: *Arctagrostis latifolia*, tundra, warming experiment, nutrient cycling, climate change, fine roots, ^{15}N tracer

Abstract

The majority of plant biomass is located belowground in Arctic ecosystems and plant roots are responsible for the uptake of the nutrients that constrain plant growth in these infertile ecosystems. Despite performing a crucial role connecting primary producers to the soil, roots are relatively understudied in the Arctic and their functional response to a rapidly warming and increasingly variable climate is unknown. We assessed whether one growing season with elevated temperatures would have an impact on nutrient uptake and allocation by applying a warming technique that increased daily air temperatures by 3.2°C. Destructive sampling was performed at the peak of the growing season to quantify biomass pools of carbon (C) and nitrogen (N), root traits, and uptake of a ^{15}N tracer ($^{15}NH_4^+$) for the dominant plant species, *Arctagrostis latifolia*. We found that soil nutrient availability increased with short-term warming but *A. latifolia* NH_4^+ uptake remained unchanged. Fine root length density and root biomass within the soil profile, however, were both reduced by warming. N allocation patterns across plant tissues were also altered by warming. NH_4^+ uptake was best fit with a logistic model that captured the spatial relationship between roots and soil (NH_4^+ uptake expressed per length fine root and NH_4^+ availability expressed per unit soil volume) rather than a traditional Michaelis-Menten model. Our results indicate that short-term experimental warming can shift plant-soil interactions, suggesting that the tundra's belowground response to elevated temperatures may be more dynamic than previously recognized.

Manuscript Highlights

- Short-term warming enhanced soil nutrients and reduced plant roots
- Plant allocation of N across tissues was increased by short-term warming
- In-situ nutrient uptake is not captured well by the Michaelis-Menten model

Introduction

Climate change has already begun to have profound effects on arctic ecosystems. Arctic regions have warmed by 3.1°C since the 1970s, roughly four times faster than lower latitude ecosystems (AMAP 2021; Rantanen and others 2022). The frequency and geographic extent of arctic heat waves have also increased since 2002 (Dobricic and others 2020). In the coming decades, mean annual temperature (MAT) in the Arctic is expected to increase by an additional 4 °C compared with 1981-2005 baseline temperatures (RCP 4.5 & 8.5; Overland *et al.*, 2014; Post *et al.*, 2019), and the hot extremes are expected in increase in both frequency and duration (Screen and others 2015). Recent observations support these trends: 2023 was the warmest arctic summer on record since 1900, and eight of the years recording the warmest arctic MAT have all occurred since 2016 (Ballinger and others 2023). The impacts of such rapid climate change on arctic ecosystems are complex and interconnected, requiring an arsenal of ecological tools to parse.

Manipulative field experiments have proven to be an important inferential tool for identifying critical mechanisms behind changes in the structure and function of arctic ecosystems. Long-term manipulative experiments have identified shifts in plant community composition in response to higher air temperatures (Elmendorf and others 2012), changes in plant and soil interactions in response to fertilization (Van Wijk and others 2003), and reduced storage of C in permafrost soils in response to elevated soil temperatures (Hicks Pries and others 2016). Due to the remote nature of field sites, energy-intensive warming experiments have been challenging to implement in the Arctic. Many have been implemented using open-top chambers or greenhouses (van Gestel and others 2019). Such passive-warming chambers, however, elevate air temperatures by only about 2°C (Chapin and others 1995; Sistla and others 2013; Hollister and others 2023) and have little impact on soil temperatures (Marion and others 1997). Long-term manipulative experiments that increase belowground temperatures present their own logistical challenges. Warmed tundra soils often thaw, subside, and collect water – no longer reflecting the landscape-scale hydrological response to warming (Rodenhizer and others 2023). Whether warming treatments impact above- or belowground temperatures, there are usually infrequent opportunities for destructive sampling in any long-term manipulative plots which can limit inference into belowground dynamics. Understanding the timing, magnitude, and mechanistic nature of plant-soil interactions and their response to warming is therefore a unique challenge in arctic ecosystems. Though short-term, high temperature warming experiments cannot yield insight into long-term responses of tundra vegetation and soils, they can inform our understanding of how quickly arctic plant-soil interactions respond to changes in temperature and the short duration of these experiments allows for the extensive destructive harvests necessary to characterize belowground responses.

Studying belowground dynamics in arctic ecosystems provides critical insights into the function, resilience, and responses of these unique and vulnerable environments to environmental change. Arctic

plants allocate a majority of their biomass belowground (Iversen and others 2015), and 93% of their roots are located in the top 30 cm of the soil profile (Jackson and others 1996) so even shallow soil warming could dramatically alter plant access to nutrients and plant C sequestration. The pace at which aboveground processes respond to warming versus belowground processes will determine plant N demand and potential allocation to roots. Meta-analyses of existing long-term, high-latitude warming experiments have generally shown progressive ecosystem responses to moderate increases in temperature: plant phenology is impacted first, then plant productivity accelerates, and finally soil N availability increases in these typically nutrient-limited ecosystems (Arft and others 1999; Rustad and others 2001; Aerts and others 2006). It is largely unknown whether responses to warming of greater magnitude will follow this same, plant-driven trajectory or how quickly belowground interactions between plants and soils might be impacted by extreme heat. The direct impacts of a warming and more variable climate on soil decomposition and nutrient cycling are highly relevant in the Arctic because access to N and phosphorus (P) can limit plant productivity as well as decomposition by the soil microbial community (Chapin 1978; Ulrich and Gersper 1978; Shaver and Chapin 1980; Shaver and others 1986; Chapin and Shaver 1996; Nadelhoffer and others 2002; Mack and others 2004). Understanding changing rhizosphere nutrient dynamics is therefore critical for predicting the future function of tundra ecosystems. Current model representations of plant access to soil nutrients often rely on kinetic parameters of enzyme-catalyzed reactions (Kuzyakov and Xu 2013), though representation of competition between plants and microbes varies widely across models (Zhu and others 2017). In arctic ecosystems specifically, Zhu *et al.* (2016) demonstrated that modeled plant uptake of N is sensitive to competition with soil microbes over available N. Little is known, however, about how quickly elevated temperatures alter soil N availability and plant uptake.

To address critical knowledge gaps around arctic N cycling and the impact of short-term, high temperature warming, we deployed a zero-power warming treatment that substantially elevates growing season air temperatures relative to ambient air temperatures (Lewin and others 2017), with subsequent impacts on surface soil temperatures. The zero-power warming chambers have internal and external heat exchangers coupled with pistons that open and close chamber vents to maintain a set temperature differential. When the interior of the chamber is warmer than the exterior of the chamber, the pistons force open the vents and the chamber cools. Similarly, if the interior of the chamber is too cool, the piston close the vents and the chamber temperature rises. This approach allows application of a strong warming treatment without the need for electrical power or risk of overheating.

The warming treatment was applied for a full arctic growing season, and the responses of soil nutrient availability as well as biomass and N uptake of a common arctic grass species (*Arctagrostis latifolia)* were quantified. The study species *A. latifolia* is a common arctic grass that thrives in mesic, disturbed

sites (McKendrick and others 1978; Ebersole 1987). It is a typical species in several wetland and graminoid tundra communities that together make up 22% of the non-glaciated area of the Arctic (Walker *et al.*, 2005; CAVM 2024 data citation). The availability of N and P colimit vegetation at our study site in Utqiaġvik, AK (Chapin III and others 1975; Ulrich and Gersper 1978). We decided to focus on N rather than P cycling because of its relevance for a broader number of nutrient-enabled earth system models (Davies-Barnard and others 2020) as well as the ability to use a stable isotope tracer (^{15}N-NH_4). We consider NH_4^+ a proxy for N cycling broadly due to rapid mineral N turnover playing an important role in low nutrient tundra systems (Ramm and others 2022) and the relative rarity of NO_3 in these soils (Norby and others 2018). Based on the warming responses of previous, milder, arctic warming experiments, we hypothesized the following three responses to short-term warming:

(H1) Short-term warming will have a limited impact on the availability of nutrients in the soil profile.

(H2) Low nutrient availability will restrict warming-induced increases in *A. latifolia* biomass.

(H3) *A. latifolia* will shift toward more acquisitive root traits to enable faster rates of N uptake from the soil.

Data from this experiment will address these hypotheses and will be used to investigate whether standard methods of describing uptake kinetics in models capture the relationship between root traits, nutrient uptake, and nutrient availability in this tundra ecosystem.

Materials & Methods

Site description

Research was conducted at the Barrow Environmental Observatory (BEO), near the town of Utqiaġvik, Alaska (71°17'N, 156°47 °W). This site is underlain by continuous permafrost and has a mean annual air temperature of -9.87°C and mean annual precipitation of 135 mm (1990-2020, NOAA 2018 data citation). The vegetation is broadly characterized as a graminoid and moss-dominated wetland (Raynolds and others 2005). The underlying nutrient-poor, Gelisol soils mean plant growth is generally limited by nutrient availability (Chapin and others 1975). Thawed lake basins and polygonal tundra are common landscape features at the BEO and soils are organic-rich and impacted by cryoturbation (Hinkel and others 2003).

Experimental design

On 16 June 2018, while the tundra was still snow-covered and average daily air temperatures were below freezing, five zero power warming (ZPW) chambers were deployed (prototype described in

Lewin *et al.*, 2017). The chambers covered a 2.4 m × 2.4 m area of ground and were 1.4 m tall. Locations for ambient plots and chamber deployment in 2018 were chosen during the 2017 growing season. Paired warmed and ambient plots were chosen to encompass similar microtopography, hydrology, and cover of *A. latifolia*. Each set of paired plots were separated from other replicate pairs by at least 16 m. ZPW chambers were removed at the end of the growth season before the ground froze (24 September 2018).

Environmental conditions

For the 100-day period when chambers were deployed, air temperature 50 cm above the canopy was continuously logged in each chamber and at one centrally located meteorological station outside the chambers (Campbell Scientific, 083E-L Met One Temperature/RH Sensor with Solar radiation shield). Soil temperature was logged continuously at 10 cm depth within the five chambers and five paired ambient plots (Campbell Scientific,109SS-L). Owing to technical difficulties, only 2 pairs of soil temperature sensors were fully functional through 11 July (DOY 192), then 4 pairs of sensors reported data for the remainder of the season. Soil volumetric water content (VWC) was measured at 5 cm depth and data were processed with standardized equations for peat soil (Decagon GS3). Continuous measurements of soil temperature, air temperature, and VWC were logged once a minute and averaged daily.

Harvests for natural abundance

On 20 July 2018 (DOY 201), 9 cm × 9 cm areas of *A. latifolia* were harvested at one location in each warmed plot and paired 'ambient' plot for determination of biomass pools and natural abundance of ^{15}N. Harvest locations were randomly selected within the plots. A serrated knife was used to cut to the bottom of the organic layer (approximately 10 cm). To sample roots and soils beneath the organic layer, a 5-cm diameter soil core was collected from within the footprint of the harvested organic layer. Soil cores spanned the bottom of the organic horizon to frozen ground. Immediately following collection, soil cores were separated into 5-cm depth intervals and each depth interval was split vertically in half. One half was set aside for assessing soil properties and one half was set aside for removal of fine roots (< 2 mm diameter). Organic horizon samples were stored in a dark refrigerator and *A. latifolia* biomass was separated from organic soils and sorted by tissue type (attached litter, blades, sheaths, inflorescences, rhizomes, new tillers, fine roots). New tillers were white, immature buds that lacked green leaves and are analogous to "V_O" tillers as classified by Shaver *et al.* (1986). *A. latifolia* tissues were separated from organic soils within 48 hours of collection and were dried at 65°C for 24 hours. All soil samples were frozen the day they were collected and were shipped to ORNL for further processing.

^{15}N-NH_4^+ label, incubation, and harvest

At two replicate locations within each plot, a trace amount of ^{15}N labeled ammonium was introduced to the soil as a ^{15}N-NH_4Cl solution (2.4 mmol ^{15}N-NH_4Cl L^{-1}; Sigma Aldrich >= 98 atom% ^{15}N, Lot # MBBC2459) on 21 July 2018 (DOY 202). We chose to label NH_4^+ for this experiment for several reasons. Tundra graminoids tend to rely heavily on organic nitrogen sources due to the slow decomposition in this ecosystem (Chapin and others 1993; Schimel and others 2004) but tracing direct uptake rates for organic N substrates can be complicated by microbial mineralization, as microbial uptake of organic N takes place within hours (Nordin and others 2004). Tundra graminoids can take up NO_3^- (nitrate) when it is available (Koch and others 1991), but tundra soils have a relatively small NO_3^- pool (Hansen and Elberling 2023) which would make even application and homogenization of the isotopic label a challenge. We injected the ^{15}N-NH_4Cl solution using a side-port spinal needle at 3 cm depth. Each labeled area was 12 cm × 12 cm and injections were performed at gridded 3-cm intervals. At each of the grid points, a 5-ml aliquot of the ^{15}N-NH_4Cl solution was injected. Test injections of food coloring showed the diffusion zone was 1.5 cm so this ensured an even application of +200 mg ^{15}N m^{-2} (similar to McKane *et al.*, 2002). After a period of 6 days, harvests were performed at the two replicate ^{15}N-labeled areas within each plot. Plants and the surface organic layer from the inner 9 cm × 9 cm of the labeled area were harvested following the protocol described above. Soil cores beneath this organic layer were similarly collected following the protocol detailed for natural abundance sampling. The 6-day incubation period with the ^{15}N-label was intended to allow not only uptake but distribution of the label throughout plant tissues and is within the typical 1 to 7 day range of tundra ^{15}N isotopic label experiments (McKane and others 2002; Zhu and others 2016; Hewitt and others 2019).

Aboveground plant traits

Prior to harvest, the maximum height of *A. latifolia* was recorded. Immediately following tissue sorting, all blade tissue samples were scanned using a leaf area scanner (LI-3100, Li-Cor Biosciences, Lincoln, Nebraska). After scanning, all samples were dried at 65 ^{0}C for 24 hours and weighed. Specific leaf area (SLA) was calculated as m^2 leaf area per g dry leaf mass. Leaf area index (LAI) was calculated as m^2 leaf per m^2 ground.

Soil core processing

At ORNL, subsamples of soil from each depth interval were weighed, dried at 70 ^{0}C for 48 hours, and reweighed for determination of gravimetric water content (GWC) and bulk density. The dried material was then ground and analyzed for %C and %N (Model 4010 Elemental Combustion System, Costech Analytical Technologies, Valencia, CA, USA). Water-extractable pools of NH_4^+, NO_3^-, Total N

(TN) and dissolved organic C (DOC) were measured on 10 g field-moist subsamples of soil. Briefly, soil subsamples were thawed, 50 ml of nanopure water was added, and the mixture was agitated for 60 mins before being vacuum extracted through Whatman GF/A filters (1.6 µm pore size). Soil extract solution was frozen prior to analysis for NH_4^+, NO_3^- and PO_4^- on a Lachat 8500 autoanalyzer (Hach Company, Loveland, CO). TN and DOC were measured on a TOC-L instrument with a TNM unit (Shimadzu, Kyoto, Japan). Inorganic N fraction was calculated as the sum of dissolved $NH_4^+$and NO_3^-divided by TN. Dissolved organic N (DON) was calculated as TN minus $NH_4^+$and NO_3^-.

Root sample processing

A. latifolia living rhizomes and fine roots (< 2 mm diameter) were removed from surface organic horizon shortly after harvest. Deeper mineral layers sampled with a soil corer were thawed in the laboratory at ORNL for fine root removal. In the field, the 5-cm diameter cores had been separated into depth intervals in the field and split in half vertically. One half of each depth interval was picked for *A. latifolia* fine roots, which were distinguished from other species visually based on vouchers collected in the field. Though we did not measure roots from non-target species, most roots in the samples belonged to the *A. latifolia* (*V. Salmon* personal observation). Live roots were differentiated from dead based on color and elasticity. After removal from the soil, live fine roots and rhizomes were rinsed with a 0.01M $CaCl_2$ solution for 30 seconds and then rinsed in deionized water to ensure removal of ^{15}N on the root surface. After rinsing, fine roots were scanned in trays of water at 1400 dpi using a flatbed scanner and WinRhizo software (Regent Instruments, Inc., Québec, Canada). Roots were carefully spread out on trays to minimize overlap. After scanning, roots were dried at 70 ^{0}C for 48 hours and weighed. Fine root length and dry mass were used to calculate specific root length (SRL; m g^{-1}; a trait specific to individual roots or groups of roots) and root length density (RLD, cm root cm^{-3} soil; the total length of roots throughout a volume of soil).

Biomass and N uptake

Blades, sheaths, inflorescences, rhizomes, new tillers, and fine roots of *A. latifolia* were dried, weighed, ground, and analyzed for ^{15}N content on an elemental analyzer-isotope ratio mass spectrometer (EA-IRMS; Integra CN, SerCon, Crewe, UK). Tissue-specific %C and %N were also analyzed on a stand-alone elemental analyzer (Costech Analytical Technologies, Inc, Valencia, CA, USA). If fine-root tissue samples were too small to run for ^{15}N, %N and %C, they were combined with fine-root samples from adjacent soil depths.

C and N biomass pools were calculated by multiplying dry mass of each tissue pool by C or N content and dividing by the ground area harvest. Values were averaged at the plot level to test for differences

between treatments (3 harvests per plot from one natural abundance harvest and two ^{15}N label harvests). For calculating N uptake, pools of ^{15}N in all harvested tissues were examined. The atom percentage ^{15}N in excess (APE, atm%) for each tissue was calculated as:

$$APE = {}^{15}N_{labeled-} - {}^{15}N_{natural\ abundance} \quad \text{(eq. 1)}$$

where $^{15}N_{labeled}$ was atom percent ^{15}N for the tissue in the ^{15}N labeled harvest and $^{15}N_{natural\ abundance}$ was atom percent ^{15}N of the tissue from the corresponding natural abundance harvest. ^{15}N uptake rate (µg ^{15}N m^{-2} hr^{-1}) during the entire incubation period was then calculated for each tissue as:

$$15N\ uptake = Tissue\ N\ x\ \frac{APE}{100}\ x\ \frac{1}{t} \quad \text{(eq. 2)}$$

where Tissue N represents tissue-specific biomass pools of N (µg N m^{-2}), and t was the incubation time in hours. ^{15}N uptake reflects only the rate of uptake for the labeled form of NH_4^+ from the soil solution and is influenced by the dilution by the total available NH_4^+ pool in the soil. We therefore calculated overall ammonium uptake (herein referred to as NH_4^+ uptake, µg N m^{-2} hr^{-1}) rate based on the following isotope mixing model (McKane and others 2002; Gallet-Budynek and others 2009):

$$NH4\ uptake = 15N\ uptake\ x\ \frac{C_{available\ N}}{C_{15N\ label}} \quad \text{(eq. 3)}$$

where $C_{available\ N}$ was the pool of water-extractable NH_4^+ in the diffusion zone where the ^{15}N label was introduced (mg N m^{-2}). $C_{available\ N}$ was calculated based on the 1.5 cm diffusion radius, bulk density, and extractable NH_4^+ pool of the surface organic soil. $C_{15N\ label}$ was the amount of ^{15}N introduced to the diffusion zone.

NH_4^+ uptake rates were calculated per g plant N (µg N g^{-1} N hr^{-1}) and as percent recovery of the introduced ^{15}N label. Both metrics of N uptake were analyzed at the plot-level based on averages from the two replicate ^{15}N labels per plot.

Nutrient availability throughout the growing season

Mixed bed exchange resins bags were used to assess availability of inorganic N and P in surface soils throughout the entire ZPW chamber deployment period. This measurement was pursued to see if a time-integrated metric of nutrient availability differed from soil-extractable nutrients sampled during harvests conducted at the peak of the growing season. Resin bags were constructed with IONAC NM-60 H+/OH- Form, Type 1, Beads (16-50 Mesh, JT Baker #4631-01). Each bag contained 10 g of wet resin

material within acid-washed nude pantyhose. Four resins were deployed per plot in July 2018 at 10 cm depth. Resins in warmed plots were deployed 9 July 2018 while resins in ambient plots deployed 14 July 2018 because of slower soil thaw. All resins were collected on 26 September 2018 and were shipped to ORNL. In the lab, resins were air-dried and then sequentially extracted 3× with fresh, 15-ml aliquots of 2 M KCl. Sequential extracts were then combined and frozen prior to analysis for NH_4^+, NO_3^-, and PO_4^- on a Lachat 8500 autoanalyzer. Final blank-corrected resin extracts were expressed µg N g dry resin^{-1} and µg P g dry resin^{-1}. Resins in warmed plots were deployed for 6 more days than ambient plots but do not represent resin-bound N and P on a per day basis because the accumulation of nutrients on resins is not linear in tundra ecosystems (Giblin and others 1994) and the deployment period reflects the impact of warming on the length of the belowground growing season.

Statistical analysis

All statistics and graphing were performed in R (R Core team, version 4.0.0; *tidyverse*, *ggplot2*). The impact of warming on environmental variables and aboveground plant traits (SLA, LAI, height) was assessed using paired t-tests performed on average values for each plot (n = 5).

The impact of the warming on C and N in tissue-specific biomass pools was tested using a two-way analysis of variance with tissue type and treatment as discrete effects. Data from three sub-replicate harvests were averaged at the plot level prior to model fitting (one natural abundance harvest and two ^{15}N label harvests). Data were transformed (log, exponential, square root, or inverse) to improve normality according to a Shapiro-Wilk normality test. The impact of warming on NH_4^+ uptake was similarly analyzed though there were only two sub-replicate harvests averaged for the plot-level data on which the model was run. For plot-level averages of soil extracts and root traits, we fit a model that included both treatment and depth interval as discrete variables. The impact of warming on resin-bound N and P pools, total plant biomass pools, and total plant uptake of NH_4^+ was assessed using a one-way analysis of variance.

A high degree of variation was observed for NH_4^+ uptake, extractable soil nutrients, and fine-root traits across the warming and ambient plots. To determine whether there were consistent relationships among these belowground observations, we performed a principle components analysis on plot-averaged observations of extractable TN, extractable P, NH_4^+ uptake, fine root SRL, fine root biomass, fine root length density, soil temperature and air temperature.

To relate our findings to kinetic parameters of nutrient uptake commonly used in biogeochemical models, we examined NH_4^+ uptake versus the observed levels of NH_4^+ in surface soils. This analysis was performed on data from individual ^{15}N subplot harvests (n=2 per plot) rather than at the plot-level to better capture the variability across the range of the observations and maintain a close spatial relationship

between nutrient uptake and soil nutrient availability. Because this deviates from our plot-based experimental design, we did not test treatment differences in the kinetic models. We instead view the conditions imposed by the treatments as a means for expanding the axes of variation captured in our data. Initially, we fit a Michaelis-Menten (MM) curve to uptake data. Uptake was expressed in μM g^{-1} fine root hr^{-1} and availability was expressed as NH_4^+ concentration of the soil solution (μM; Kuzyakov and Xu 2013). NH_4^+ availability was calculated based on soil extract concentrations, bulk density, and GWC. Uptake rates used the fine roots found in the 0-10 cm horizon because this was the depth interval in which the ^{15}N label was applied. The MM model fit was extremely weak, so we explored transforming the data to alternate units and found a strong relationship between NH_4^+ uptake per length fine root (again from 0-10 cm horizon) and NH_4^+ availability per cm^3 of soil. A logistic model was fit to this data. We reported both MM and logistic model fits with 95% confidence intervals for parameters based on bootstrapping (1000 iterations).

Results

Warming increased air temperatures most in early growing season

ZPW chambers were deployed for the 2018 growing season (16 June 2018 – 24 September 2018). The growing season was defined based on ambient conditions at the site and reflects historic patterns of aboveground plant productivity. During the growing season deployment period, the chambers increased daily air temperatures by an average of 3.2°C (Figure 1a, $p < 0.0001$). The impact of the ZPW on daily average air temperatures ranged from -0.1°C to 12.1°C (standard deviation 2.4°C, standard error of 0.1°C) across the entire deployment period. Mean air temperatures in the ambient plots were 3.3°C (± 0.2°C standard error) while mean air temperatures in the ZPW chambers were 6.5°C (± 0.2°C standard error). There was a seasonal pattern in the impact of the ZPW on air temperature: early in the growing season when solar energy input was the greatest, the ZPW chambers increased air temperatures more than they did at the end of the growing season. In June, air temperatures were elevated by 6.9°C, but in September air temperatures were elevated by only 1.6°C, potentially due to changing sun angles during the Arctic growing season. From the start of the ZPW chamber deployment (16 June 2018, DOY 167) through to the application of the ^{15}N label (21 July 2018, DOY 202), the average air temperature in ZPW chambers was increased by 5.4°C. In all months of the growing season, the change in air temperature from ZPW was significantly greater than zero ($p < 0.0001$).

Soil temperatures at 10 cm were only slightly impacted by warming treatment in the latter half of the growing season and exhibited a high degree of heterogeneity throughout the summer (Figure 1b). The average difference in daily soil temperature throughout the deployment period tended to be higher than zero (0.5°C, $p = 0.10$). On a month-by-month basis, we saw that the change in soil temperature in warmed

plots was not significantly greater than zero in June and July, potentially because of lower data availability during this period. In August and September, soil temperature at 10 cm was 0.5°C and 0.6°C higher in warmed plots ($p = 0.10$ and $p = 0.05$ respectively). Prior to the application of the ^{15}N label, the warming increased the average soil temperature by 0.6°C ($p = 0.13$). There was notable periodicity seen in the soil temperature offsets associated with the ZPW chambers (Figure 1b) which could be due to warm rain events impacting ambient plots. Soil VWC was variable because of differences in plot topography but was not significantly impacted by the warming treatment despite the ZPW's interception of incoming summer precipitation (not shown). At this site, the shallow water table is perched on permafrost and lateral flow into and out of the plots ensured the warmed plots were hydrologically connected to the surrounding landscape (Lewin *et al.*, 2017).

Nutrient availability increased with warming

Soil nutrient availability increased significantly with summer warming when measured using both soil water extracts and resins. The three extractable N pools measured (TN, inorganic N fraction, and DON) all significantly increased with warming (Figure 2a, b & c). Depth, as a discrete variable, impacted TN and inorganic N fraction but not DON. The strong impact of warming in 0-10 cm soil on TN (Figure 2a) was driven by an increase in the inorganic N fraction in surface soils (Figure 2b) rather than DON (Figure 2c). Extractable P was similarly highest in the surface soils of warmed plots (Figure 2d) and was also the only extractable pool that exhibited a significant interaction between depth and warming. This interaction stems from deep soils in warmed plots having lower extractable P than deep soils in ambient plots. Warming also significantly elevated pools of extractable DOC (Figure 2e). The surface organic horizons of warmed plots all had notably higher magnitude and variation of extractable TN, extractable P, and extractable DOC compared to mineral soils (Figure 2a, 2d, and 2e).

Ion-exchange resins deployed throughout the growing season also showed increased soil nutrient availability with warming, as they bound significantly more inorganic N and P within warmed plots (Figure 3). Warming nearly tripled resin total inorganic N (TIN; Figure 3c), driven by a seven-fold increase in NO_3^-(Figure 3a). Resin P increased with warming ($p = 0.06$) and the magnitude of this increase was similar in scale to that of NO_3^-.

Warming increased aboveground C:N but had no impact on plant C or N pools

Warming had no significant effect on C in total biomass C or N pools (Table 1) but this could not be attributed to low N availability (Figure 2, 3). The C:N of aboveground tissues, however, did increase with warming (Table 1, $p = 0.07$). The change in C:N aboveground was driven by increases in the C:N of inflorescences and new tillers in warmed plots ($p = 0.01$, $p = 0.09$ respectively). The C:N of blades was

not impacted by warming. The higher C:N of aboveground plant biomass was caused by a non-significant increase in aboveground C pools without a concurrent change in aboveground N pools (Table 1). Neither SLA nor LAI were significantly impacted by warming, though the maximum height of *A. latifolia* was greater in warmed plots by 40% or 6.5 cm (Table 2, $p = 0.03$).

Whole-plant uptake of NH_4^+ not impacted by warming despite altering fine-root traits

Whole-plant uptake of NH_4^+ did not increase with warming (Figure 4) and there was a negative warming effect on several acquisitive root traits (Figure 5). Both root length per unit soil volume (root length density, RLD) and biomass per unit ground area declined with soil depth and were reduced in response to warming (Figure 5, a & b). The specific root length (SRL, m g^{-1}) of fine roots increased with depth but did not respond to warming (Figure 5c). Fine root C:N decreased with depth and was unresponsive to warming (Figure 5d). The overall negative impact of warming on root length and mass did not impact rates of whole-plant NH_4^+ uptake or recovery of the isotopic label (Figure 4, a & c, $p = 0.46$ and $p = 0.53$). Interestingly, when NH_4^+ uptake was examined per tissue pool, warming tended to be associated with faster uptake (Figure 4b, $p = 0.08$) as well as higher recovery of the ^{15}N label (Figure 4d, $p = 0.05$). Warming was associated with higher variation in both these metrics of NH_4^+ uptake which likely obscured treatment effects when summed for the whole-plant response. The high degree of variation in NH_4^+ uptake, root traits, and soil nutrient availability was explored with a principal components analysis (Figure S1, Table S1). PC1 explained 41.3% of the observed variation and was highly influenced by extractable TN, extractable P, and NH_4^+ uptake. PC2 explained 29.2% of the observed variation and was influenced to a greater degree by fine-root traits (SRL, biomass, and length density). Soil- and air temperature were only moderately weighted in PC1 and PC2, with soil temperature being more influential for PC1 and air temperature being more influential for PC2.

Kinetics of NH_4^+ uptake

Fitting a MM model to our data was not successful: NH_4^+ uptake and NH_4^+ availability did not exhibit a hyperbolic shape when expressed in units commonly used for this purpose (Figure 6a). V_{max} and K_m parameters therefore had large confidence intervals that crossed zero. A logistic model fit to NH_4^+ uptake expressed per m fine root (µg N m^{-1} fine root h^{-1}) and water extractable NH_4^+ per unit soil volume (µg N cm^{-3} soil), however, fit well (Figure 6b). Bootstrapping the logistic model showed the rate of NH_4^+ uptake plateaus at 0.19 µg N m^{-1} h^{-1} (parameter a, 95% CI from 0.17 to 0.21) and is most efficient when soil NH_4^+ availability is 4.12 µg N cm^{-3} soil (parameter c, 95% CI from 3.81 to 4.42). The steepest slope along the line equals 0.069 cm^3 m^{-1} hr^{-1} (calculated as $a \times (|b|/4)$ based on the derivative of the curve).

Discussion

Our study found N and P availability in tundra surface soils increases when the ecosystem is exposed to short-term warming. The warming treatment was applied using self-venting ZPW chambers that elevated air temperatures by 3.2°C, much stronger than the warming associated with commonly used open top chambers (1.2-1.8 C, Marion and others 1997). Warming decreased fine-root length and fine-root biomass of *A. latifolia* when these traits were examined within the soil profile, but warming did not result in a change to whole-plant NH_4^+ uptake or biomass C & N pools. Allocation of the isotopic label among plant tissues tended to be greater with warming but exhibited a high degree of variability. Most notably, our results suggest the belowground dynamics among plant C, soil N availability, and NH_4^+ uptake can change rapidly with warming. Capturing the dynamics of in-situ nutrient uptake is best approached using a logistic curve fit to NH_4^+ uptake rates expressed per m fine root and NH_4^+ availability expressed per cm^3 soil volume rather than a traditional Michaelis-Menten model.

Tradeoffs between nutrient availability and fine roots supports allocation theory

In contrast with our hypothesis that short-term warming would not be sufficient to increase soil nutrients (H1), both peak-season soil extracts and seasonal resins showed warming increased soil nutrient availability. Extractable P pools in surface soils increased by an order of magnitude and extractable TN increased by a factor of 3 with warming. The differential impact on nutrients in surface soils could be attributed to warming having a greater impact on shallow soil temperatures (Lewin and others 2017). The inorganic N fraction was highest in warmed surface soils, indicating increased net N mineralization. The high extractable P pool in the organic horizon (0 – 10 cm) is likely from mineralization of P previously bound in organic matter while deeper in the soil a greater portion of extractable P might have come from mineral surfaces. Because we used water as an extract rather than a salt solution, we likely did not release a large portion of mineral-sorbed P. The strong warming effect on shallow, extractable P might also reflect the stimulation of both plant and microbial phosphatases. In addition to increasing N and P availability, warming also altered the balance of inorganic N forms bound to resins. The increase in TIN bound to resins at the end of the growing season was driven by an increase in NO_3^- rather than NH_4^+. Resin data therefore suggest a warming-induced increase in nitrification, a process often overlooked in arctic soils despite evidence of plant NO_3^- acquisition (Liu and others 2018). Soil water extracts at peak growing season, in contrast, showed an increase in both forms of inorganic N. The discrepancy between warming's impact on NH_4^+ and NO_3^- measured with resins versus soil extracts could be attributed to a late-season increase in nitrification that would have impacted resin ammonium pools (collected in September) but not soil-extractable pools (collected in August). Late season nitrification has been observed in other tundra studies (Treat and others 2016; McLaren and others 2017). Our results support a growing body of

literature suggesting that mineral N transformations are a small but dynamic part of the tundra nutrient cycle (Ramm and others 2022) and demonstrates that the availability of limiting nutrients in tundra soils can increase rapidly in response to warming.

In conjunction with the warming-induced increase in nutrient availability, the length and mass of *A. latifolia* roots decreased. We hypothesized that *A. latifolia* roots traits would change with warming (H3), but we anticipated this would involve an increase in traits associated with nutrient acquisition in response to increasing plant demand for nutrients and a static N pool in the soil. Instead, we found that soil nutrient availability increased while root quantity decreased and whole-plant NH_4^+ uptake by *A. latifolia* remained static. This tradeoff between nutrient availability and *A. latifolia* fine roots was visible in the PCA (Figure S1): PC1 captured metrics of soil nutrient availability and uptake while PC2 captured root traits. Within PC1, increases in nutrient variables were associated with decreases in fine root length and SRL (Table S1). Allocation theory predicts decreased allocation to fine roots when belowground resources is in excess (Bloom and others 1985). This theory is supported by observations: decreased allocation to fine-root productivity in response to accelerated nutrient cycling has been observed in warmed temperate systems (Melillo and others 2011) and tundra plants fertilized at high levels for 7 years (10 g N m^{-2} y^{-1} and 5 g P m^{-2} y^{-1}; Nadelhoffer *et al.*, 2002). The link between warming and decreased root allocation is not ubiquitous, however: warming experiments across the globe tend to increase fine-root production and biomass (Wang and others 2021) and similar patterns have been seen in tundra ecosystems warmed for one year (Sullivan and Welker 2005). Our single-species, short-term results may indicate weaker N and P limitation in Utqiaġvik relative to other tundra sites but conservative cycling of these two elements has been well documented at this site (Chapin 1978; Ulrich and Gersper 1978). Alternatively, our results may indicate a difference in short versus long-term plant response to altered environmental conditions. This study focused on a single species rather than the belowground response of the whole plant community and was limited to a single growing season. Nutrient limitation of plant productivity and control over acquisitive root traits may still be important if the plant community were to shift toward species over a longer warming period. Such long-term community dynamics, however, are outside the scope of this experiment but do merit further investigation.

N allocation across tissues is sensitive to warming but highly variable

Our observations supported our hypothesis (H2) that biomass pools of *A. latifolia* would not increase with a single season of warming though this response could not be attributed to nutrient limitation. Our data did, however, provide insights into how N allocation across different tissue pools responds to short-term warming. Tissue-specific C:N, NH_4^+ uptake, and recovery of the ^{15}N label were all sensitive to warming despite these metrics exhibiting a non-significant response when the tissues were

summed up for a whole-plant response. We attribute the discrepancy in the warming responses of whole-plants versus tissues to the high degree of variability seen across tissue and within the warmed plots. There were also notable differences in the tissue-specific warming responses of these allocation metrics.

Warming increased the C:N of inflorescences and new tiller sprouts developing belowground. Higher C:N ratios have been associated with later stages of annual tissue development due to changing allocation of C versus N through time (Welker and others 2005). Because inflorescences and new tillers were actively maturing at the time of our peak-season sampling, the observed increase in inflorescence and new tiller C:N may be explained by warmed plots having an earlier start to the growing season. Our experiment similarly had a three-day earlier onset of greenup in warmed plots (McMahon et al., 2024 dataset, Table S2, $p = 0.06$). Arctic warming experiments have broadly been associated with earlier bud break, flowering dates, and reproductive effort (Arft and others 1999; Klady and others 2011; Natali and others 2012). Arctic warming has also been shown to increase plant height (Bjorkman and others 2018) which is consistent with the increase in canopy height we observed. In contrast to biomass C:N, warming had the greatest impact on tissue-specific NH_4^+ uptake and recovery of the ^{15}N label in rhizomes and fine roots. Belowground allocation of recently acquired NH_4^+ at this single timepoint July could be attributed to belowground productivity lagging behind aboveground productivity in tundra ecosystems (Gallois and others 2025). Alternatively, rapid turnover of fine roots (McCormack and others 2015) and the tendency of tundra plants to store large amounts of nutrients in rhizomes (Iversen and others 2015) could explain why allocation to these tissues is more sensitive to warming. If warming conditions were to extend to longer timeframes, these differences in allocation could result in change to plant N pools and demand that were not visible during our short-term experiment.

Implications for modeling nutrient dynamics

Findings from this study have several implications for modeling nutrient uptake. The warming-induced changes in trait tradeoffs suggest that microbial competition in the rhizosphere can have an important influence on NH_4^+ uptake. This supports the findings of Zhu *et al.*, (2016) who incorporated competitive interactions between plant roots and microbes in their equilibrium chemistry approximation (ECA) framework within the ecosystem land model (ELM). Several models, including ELM-ECA, rely on empirically-derived kinetic parameters to represent plant uptake of nutrients. When we looked at the relationship between NH_4^+ uptake and availability in our data, however, we found evidence that this approach to parameterizing nutrient uptake should be taken cautiously. The strongest and most consistent relationship in our data was found when uptake was expressed per length fine root and availability was expressed per soil volume. We attribute this to the fact that the interaction between plant roots and the

available nutrient pool is dependent on the spatial structure of the root-soil system. The relationship between uptake and availability fell along a logistic curve rather than a MM saturating curve, which was surprising because half saturation constants (K_m) from MM curves frequently serve as the backbone for mechanistic models of nutrient uptake (Hopmans and Bristow 2002; Rogers and Gibon 2009). Our study's logistic curve might differ from the MM curve because we measured nutrient uptake and availability of an in-situ ecosystem rather than an aquatic plant-soil system or fungal culture (McRoy and Alexander 1975; Jongbloed and others 1991). Our observations were also made over a 6-day period, which means in addition to nutrient uptake, turnover of the available N pool and microbial community presumably took place. In a complex soil system, it seems likely that uptake would depend on not only these processes but also movement of solution through the soil via simple diffusion to the root surface (McMurtrie and Näsholm 2018) or lateral flow (which we infer is important at our shallowly thawed site given the warming treatments failure to decrease soil moisture). We believe the poor fit of the MM model to our data also supports work by Rastetter & Shaver (1992) indicating the rate of nutrient supply might be a better predictor of plant uptake than the nutrient concentration when in nutrient-limited soils. Our study was based on a single species, site, and season, so further research is needed to fully understand the relationship between nutrient pool sizes, turnover, and acquisition by fine roots.

Conclusions

Short-term warming was sufficient to alter biogeochemical interactions in the tundra rhizosphere and the results presented here stand in contrast to what we might have expected given the results from longer term, milder warming experiments in the tundra. Soil nutrient availability increased dramatically within a few months of warming, but root length density and biomass across the soil profile decreased and there was no impact on whole-plant uptake of NH_4^+. These altered plant-soil interactions were paired with significant impacts of warming on plant height and allocation of N across plant tissues. When the kinetic relationship between NH_4^+ uptake and availability was examined, our in-situ nutrient uptake rates did not exhibit classic Michaelis-Menten dynamics that are integral to many plant-soil models. Plant-soil interactions in rapidly warming tundra ecosystems may be more sensitive to temperature than previously recognized and new modeling approaches may be required to accurately predict these belowground dynamics. Our results also highlight the need for more research on belowground responses to short versus long term warming and the impact of species interactions on nutrient allocation and uptake.

Acknowledgements

Authors have no conflict of interest. The land this research was performed on is part of the Barrow Environmental Observatory (BEO) and is managed by UIC science. As an Alaska native corporation, UIC

science represents the continuing stewardship of the Iñupiaq people in the region, and we thank them not only for permission to work on the land but also for the crucial logistical support they provided to this project. Additional help was provided by Dan Stover, Andrew McMahon, Kenneth Davidson, Ella Johnson, Abbygail Ochs, Deanne Brice, Geoff Schwaner, Stan Wullschleger, and Sue Heinz. This paper is dedicated to the memory of Joanne Childs: she was an integral part of the field and laboratory work presented in this manuscript. Her memory, laughter, scientific insight, and friendship will forever be cherished.

Funding

This research was conducted as part of the NGEE Arctic project, funded by United States Department of Energy's Office of Science, Biological and Environmental Research program (https://ngee-arctic.ornl.gov). Researchers associated with Oak Ridge National Laboratory (VGS, JC, BS, RN, CMI) were supported by the United States Department of Energy contract No. DE-AC05-00OR22725 to UT-Battelle, LLC. AR and KE were supported by contracts No. DE-SC0012704 to Brookhaven National Laboratory and No. DE-AC02-05CH11231 to Lawrence Berkeley National Laboratory.

Data Availability & Software Tools

R Core Team (2020). R: A language and environment for statistical computing. R Foundation for Statistical Computing, Vienna, Austria. URL https://www.R-project.org/

ggbiplot. Vincent Q. Vu (2011). ggbiplot: A ggplot2 based biplot. R package version 0.55. http://github.com/vqv/ggbiplot

ggplot2. H. Wickham. ggplot2: Elegant Graphics for Data Analysis. Springer-Verlag New York, 2016.

HH. Richard M. Heiberger (2020). HH: Statistical Analysis and Data Display: Heiberger and Holland. R package version 3.1-43. https://CRAN.R-project.org/package=HH

tidyverse. Wickham et al., (2019). Welcome to the tidyverse. Journal of Open Source Software, 4(43), 1686, https://doi.org/10.21105/joss.01686

Menne, Matthew J., Imke Durre, Bryant Korzeniewski, Shelley McNeal, Kristy Thomas, Xungang Yin, Steven Anthony, Ron Ray, Russell S. Vose, Byron E.Gleason, and Tamara G. Houston (2012): Global

Historical Climatology Network - Daily (GHCN-Daily), Version 3. Barrow Airport Daily (Station USW00027502). NOAA National Climatic Data Center. doi:10.7289/V5D21VHZ [accessed 29 Jan 2021].

Martha Raynolds, Donald A Walker, & Jana Peirce. (2024). *Raster Circumpolar Arctic Vegetation Map - 2024 Print Version*. Arctic Data Center. doi:10.18739/A2RX93F75.

Verity Salmon, Joanne Childs, Colleen Iversen, Breann Spencer, Alistair Rogers, Kim Ely, Shawn Serbin. 2021. Vegetation Warming Experiment: 15N Uptake Experiment Arctagrostis latifolia 15N Uptake, Utqiagvik (Barrow), Alaska, 2018. Next Generation Ecosystem Experiments Arctic Data Collection, Oak Ridge National Laboratory, U.S. Department of Energy, Oak Ridge, Tennessee, USA. https://doi.org/10.5440/1784751.

Verity Salmon, Joanne Childs, Colleen Iversen, Breann Spencer, Alistair Rogers, Kim Ely, Shawn Serbin. 2021. Vegetation Warming Experiment: 15N Uptake Experiment Water-Extractable Soil Nutrients, Utqiagvik (Barrow), Alaska, 2018. Next Generation Ecosystem Experiments Arctic Data Collection, Oak Ridge National Laboratory, U.S. Department of Energy, Oak Ridge, Tennessee, USA. https://doi.org/10.5440/1784755.

Verity Salmon, Joanne Childs, Colleen Iversen, Breann Spencer, Alistair Rogers, Kim Ely, Shawn Serbin. 2021. Vegetation Warming Experiment: 15N Uptake Experiment Arctagrostis latifolia Root Traits, Utqiagvik (Barrow), Alaska, 2018. Next Generation Ecosystem Experiments Arctic Data Collection, Oak Ridge National Laboratory, U.S. Department of Energy, Oak Ridge, Tennessee, USA. https://doi.org/10.5440/1784749

Verity Salmon, Joanne Childs, Colleen Iversen, Breann Spencer, Alistair Rogers, Kim Ely, Shawn Serbin. 2021. Vegetation Warming Experiment: 15N Uptake Experiment Arctagrostis latifolia Biomass and Chemistry, Utqiagvik (Barrow), Alaska, 2018. Next Generation Ecosystem Experiments Arctic Data Collection, Oak Ridge National Laboratory, U.S. Department of Energy, Oak Ridge, Tennessee, USA. https://doi.org/10.5440/1784750

Verity Salmon, Joanne Childs, Colleen Iversen, Breann Spencer, Alistair Rogers, Kim Ely, Shawn Serbin. 2021. Vegetation Warming Experiment: 15N Uptake Experiment Inorganic Nitrogen and Phosphorus on Resins, Utqiagvik (Barrow), Alaska, 2018. Next Generation Ecosystem Experiments Arctic Data

Collection, Oak Ridge National Laboratory, U.S. Department of Energy, Oak Ridge, Tennessee, USA. https://doi.org/10.5440/1784752

Verity Salmon, Joanne Childs, Colleen Iversen, Breann Spencer, Alistair Rogers, Kim Ely, Shawn Serbin. 2021. Vegetation Warming Experiment: 15N Uptake Experiment Arctagrostis latifolia Canopy Traits, Utqiagvik (Barrow), Alaska, 2018. Next Generation Ecosystem Experiments Arctic Data Collection, Oak Ridge National Laboratory, U.S. Department of Energy, Oak Ridge, Tennessee, USA. https://doi.org/10.5440/1784759

Verity Salmon, Joanne Childs, Colleen Iversen, Breann Spencer, Alistair Rogers, Kim Ely, Shawn Serbin. 2021. Vegetation Warming Experiment: 15N Uptake Experiment Environmental Observations and Thaw Depth, Utqiagvik (Barrow), Alaska, 2018. Next Generation Ecosystem Experiments Arctic Data Collection, Oak Ridge National Laboratory, U.S. Department of Energy, Oak Ridge, Tennessee, USA. https://doi.org/10.5440/1784757

Rogers A ; Ely K ; Serbin S (2024): Vegetation Warming Experiment: Thaw Depth and dGPS locations, Barrow, Alaska, 2018. Next-Generation Ecosystem Experiments (NGEE) Arctic, ESS-DIVE repository. https://doi.org/10.5440/1523844

McMahon A ; Ely K ; Serbin S ; Lewin K ; Rogers A (2024): Vegetation Warming Experiment: Environmental Conditions, Utqiagvik (Barrow), Alaska, 2018. Next-Generation Ecosystem Experiments (NGEE) Arctic, ESS-DIVE repository. https://doi.org/10.5440/2284082

References

Aerts R, Cornelissen JHC, Dorrepaal E. 2006. Plant performance in a warmer world: general responses of plants from cold, northern biomes and the importance of winter and spring events. Plant Ecology 182:65–77.

AMAP. 2021. AMAP Arctic Climate Change Update 2021: Key Trends and Impacts. Tromsø, Norway: Arctic Monitoring and Assessment Programme (AMAP) https://www.amap.no/documents/doc/amap-arctic-climate-change-update-2021-key-trends-and-impacts/3594. Last accessed 13/09/2022

667 Arft AM, Walker MD, Gurevitch J, Alatalo JM, Bret-Harte MS, Dale M, Diemer M, Gugerli F, Henry
668 GHR, Jones MH, Hollister RD, Jónsdóttir IS, Laine K, Lévesque E, Marion GM, Molau U,
669 MØlgaard P, Nordenhäll U, Raszhivin V, Robinson CH, Starr G, Stenström A, Stenström M,
670 Totland, Turner PL, Walker LJ, Webber PJ, Welker JM, Wookey P a. 1999. Responses of Tundra
671 plants to experimental warming: Meta-analysis of the International Tundra Experiment.
672 Ecological Monographs 69:491–511.

673 Ballinger TJ, Bigaalke S, Walsh JE, Brettschneider B, Thoman RL, Bhatt US, Hanna E, Hanssen-Bauer S,
674 Kim SJ, Overland JE, Wang M. 2023. NOAA Arctic Report Card 2023: Surface Air Temperature.
675 NOAA https://doi.org/10.25923/x3ta-6e63

676 Bjorkman AD, Myers-Smith IH, Elmendorf SC, Normand S, Rüger N, Beck PSA, Blach-Overgaard A,
677 Blok D, Cornelissen JHC, Forbes BC, Georges D, Goetz SJ, Guay KC, Henry GHR,
678 HilleRisLambers J, Hollister RD, Karger DN, Kattge J, Manning P, Prevéy JS, Rixen C,
679 Schaepman-Strub G, Thomas HJD, Vellend M, Wilmking M, Wipf S, Carbognani M, Hermanutz
680 L, Lévesque E, Molau U, Petraglia A, Soudzilovskaia NA, Spasojevic MJ, Tomaselli M, Vowles
681 T, Alatalo JM, Alexander HD, Anadon-Rosell A, Angers-Blondin S, te Beest M, Berner L, Björk
682 RG, Buchwal A, Buras A, Christie K, Cooper EJ, Dullinger S, Elberling B, Eskelinen A, Frei ER,
683 Grau O, Grogan P, Hallinger M, Harper KA, Heijmans MMPD, Hudson J, Hülber K,
684 Iturrate-Garcia M, Iversen CM, Jaroszynska F, Johnstone JF, Jørgensen RH, Kaarlejärvi E, Klady
685 R, Kuleza S, Kulonen A, Lamarque LJ, Lantz T, Little CJ, Speed JDM, Michelsen A, Milbau A,
686 Nabe-Nielsen J, Nielsen SS, Ninot JM, Oberbauer SF, Olofsson J, Onipchenko VG, Rumpf SB,
687 Semenchuk P, Shetti R, Collier LS, Street LE, Suding KN, Tape KD, Trant A, Treier UA,
688 Tremblay J-P, Tremblay M, Venn S, Weijers S, Zamin T, Boulanger-Lapointe N, Gould WA, Hik
689 DS, Hofgaard A, Jónsdóttir IS, Jorgenson J, et al. 2018. Plant functional trait change across a
690 warming tundra biome. Nature. http://www.nature.com/articles/s41586-018-0563-7

691 Bloom AJ, Chapin FS, Mooney HA. 1985. Resource Limitation in Plants--An Economic Analogy. Annual
692 Review of Ecology and Systematics 16:363–92.

693 Chapin FS. 1978. Phosphate Uptake and Nutrient Utilization by Barrow Tundra Vegetation. In: Tieszen
694 LL, editor. Vegetation and Production Ecology of an Alaskan Arctic Tundra. New York, NY:
695 Springer. pp 483–507. https://doi.org/10.1007/978-1-4612-6307-4_21. Last accessed 15/03/2024

696 Chapin FS, Cleve KV, Tieszen LL. 1975. Seasonal Nutrient Dynamics of Tundra Vegetation at Barrow,
697 Alaska. Arctic and Alpine Research 7:209.

698 Chapin FS, Moilanen L, Kielland K. 1993. Preferential use of organic nitrogen for growth by a
699 non-mycorrhizal arctic sedge. Nature 361.

700 Chapin FS, Shaver GR. 1996. Physiological and growth responses of arctic plants to a field experiment
701 simulating climatic change. Ecology 77:822–40.

702 Chapin FS, Shaver GR, Giblin AE, Nadelhoffer KJ, Laundre A, Laundre J a, Laundre A. 1995. Responses
703 of arctic tundra to experimental and observed changes in climate. Ecology 76:694–711.

704 Chapin III FS, Van Cleve K, Tieszen LL. 1975. Seasonal Nutrient Dynamics of Tundra Vegetation at
705 Barrow, Alaska. Arctic and Alpine Research 7:209–26.

706 Davies-Barnard T, Meyerholt J, Zaehle S, Friedlingstein P, Fan Y, Fisher RA, Jones CD, Lee H, Peano D.
707 2020. Nitrogen Cycling in CMIP6 Land Surface Models : Progress and Limitations. :1–32.

708 Dobricic S, Russo S, Pozzoli L, Wilson J, Vignati E. 2020. Increasing occurrence of heat waves in the
709 terrestrial Arctic. Environ Res Lett 15:024022.

710 Ebersole JJ. 1987. Short-Term Vegetation Recovery at an Alaskan Arctic Coastal Plain Site. Arctic and
711 Alpine Research 19:442–50.

712 Elmendorf SC, Henry GHR, Hollister RD, Björk RG, Bjorkman AD, Callaghan TV, Collier LS, Cooper
713 EJ, Cornelissen JHC, Day TA, Fosaa AM, Gould WA, Grétarsdóttir J, Harte J, Hermanutz L, Hik
714 DS, Hofgaard A, Jarrad F, Jónsdóttir IS, Keuper F, Klanderud K, Klein JA, Koh S, Kudo G, Lang
715 SI, Loewen V, May JL, Mercado J, Michelsen A, Molau U, Myers-Smith IH, Oberbauer SF,
716 Pieper S, Post E, Rixen C, Robinson CH, Schmidt NM, Shaver GR, Stenström A, Tolvanen A,
717 Totland Ø, Troxler T, Wahren CH, Webber PJ, Welker JM, Wookey PA. 2012. Global assessment
718 of experimental climate warming on tundra vegetation: Heterogeneity over space and time.
719 Ecology Letters 15:164–75.

720 Gallet-Budynek A, Brzostek E, Rodgers VL, Talbot JM, Hyzy S, Finzi AC. 2009. Intact amino acid
721 uptake by northern hardwood and conifer trees. Oecologia 160:129–38.

722 Gallois EC, Myers-Smith IH, Iversen CM, Salmon VG, Turner LL, An R, Elmendorf SC, Collins CG,
723 Anderson MJR, Young A, Pilkinton L, Blume-Werry G, Grenier M, Fälthammar-de Jong G,
724 Althuizen IHJ, Christiansen CT, Lang SI, Elphinstone C, Henry GHR, Rammell N, Mack MC,
725 See C, Rixen C, Hollister RD. 2025. Tundra Vegetation Community Type, Not Microclimate,
726 Controls Asynchrony of Above- and Below-Ground Phenology. Global Change Biology
727 31:e70153.

728 van Gestel N, Natali S, Andriuzzi W, Chapin FS, Ludwig S, Moore JC, Pressler Y, Salmon V, Schuur T,
729 Simpson R, Wall DH. 2019. Chapter 15 - Long-term warming research in high-latitude
730 ecosystems: Responses from polar ecosystems and implications for future climate. In: Mohan JE,
731 editor. Ecosystem Consequences of Soil Warming. Academic Press. pp 441–87.
732 https://www.sciencedirect.com/science/article/pii/B9780128134931000168. Last accessed
733 27/04/2021

734 Giblin AE, Laundre JA, Nadelhoffer KJ, Shaver GR. 1994. Measuring nutrient availability in arctic soils
735 using ion exchange resins: a field test. Soil Science Society of America Journal 58:1154.

Hansen HFE, Elberling B. 2023. Spatial Distribution of Bioavailable Inorganic Nitrogen From Thawing Permafrost. Global Biogeochemical Cycles 37:e2022GB007589.

Hewitt RE, Taylor DL, Genet H, McGuire AD, Mack MC. 2019. Below-ground plant traits influence tundra plant acquisition of newly thawed permafrost nitrogen. Mariotte P, editor. Journal of Ecology 107:950–62.

Hicks Pries CE, Schuur EAGG, Natali SM, Crummer KG. 2016. Old soil carbon losses increase with ecosystem respiration in experimentally thawed tundra. Nature Climate Change 6:214–8.

Hinkel KM, Eisner WR, Bockheim JG, Nelson FE, Peterson KM, Dai X. 2003. Spatial Extent, Age, and Carbon Stocks in Drained Thaw Lake Basins on the Barrow Peninsula, Alaska. Arctic, Antarctic, and Alpine Research 35:291–300.

Hollister RD, Elphinstone C, Henry GHR, Bjorkman AD, Klanderud K, Björk RG, Björkman MP, Bokhorst S, Carbognani M, Cooper EJ, Dorrepaal E, Elmendorf SC, Fetcher N, Gallois EC, Guðmundsson J, Healey NC, Jónsdóttir IS, Klarenberg IJ, Oberbauer SF, Macek P, May JL, Mereghetti A, Molau U, Petraglia A, Rinnan R, Rixen C, Wookey PA. 2023. A review of open top chamber (OTC) performance across the ITEX Network. Arctic Science 9:331–44.

Hopmans JW, Bristow KL. 2002. Current Capabilities and Future Needs of Root Water and Nutrient Uptake Modeling. In: Sparks DL, editor. Advances in Agronomy. Vol. 77. Advances in Agronomy. Academic Press. pp 103–83. https://www.sciencedirect.com/science/article/pii/S0065211302770144. Last accessed 23/04/2021

Iversen CM, Sloan VL, Sullivan PF, Euskirchen ES, McGuire AD, Norby RJ, Walker AP, Warren JM, Wullschleger SD. 2015. The unseen iceberg: plant roots in arctic tundra. New Phytologist 205:34–58.

758 Jackson RB, Canadell J, Ehleringer JR, Mooney HA, Sala OE, Schulze ED. 1996. A global analysis of
759 root distributions for terrestrial biomes. Oecologia 108:389–411.

760 Jongbloed RH, Clement JM a. M, Borst-Pauwels GWFH. 1991. Kinetics of NH4+ and K+ uptake by
761 ectomycorrhizal fungi. Effect of NH4+ on K+ uptake. Physiologia Plantarum 83:427–32.

762 Klady RA, Henry GHR, Lemay V. 2011. Changes in high arctic tundra plant reproduction in response to
763 long-term experimental warming. Global Change Biology 17:1611–24.

764 Koch GW, Bloom AJ, Chapin III FS. 1991. Oecologia Ammonium and nitrate as nitrogen sources in two
765 Eriophorum species. :570–3.

766 Kuzyakov Y, Xu X. 2013. Competition between roots and microorganisms for nitrogen: mechanisms and
767 ecological relevance. New Phytologist 198:656–69.

768 Lewin KF, McMahon AM, Ely KS, Serbin SP, Rogers A. 2017. A zero-power warming chamber for
769 investigating plant responses to rising temperature. Biogeosciences 14:4071–83.

770 Liu X-Y, Koba K, Koyama LA, Hobbie SE, Weiss MS, Inagaki Y, Shaver GR, Giblin AE, Hobara S,
771 Nadelhoffer KJ, Sommerkorn M, Rastetter EB, Kling GW, Laundre JA, Yano Y, Makabe A, Yano
772 M, Liu C-Q. 2018. Nitrate is an important nitrogen source for Arctic tundra plants. Proceedings
773 of the National Academy of Sciences 115:3398–403.

774 Mack MC, Schuur EAG, Bret-Harte MS, Shaver GR, Chapin FS. 2004. Ecosystem carbon storage in
775 arctic tundra reduced by long-term nutrient fertilization. Nature 431:440–3.

776 Marion GMG, Henry GGHRG, Freckman DDWD, JOHNSTONE J, Jones G, JONES MMH,
777 LÉVESQUE E, MOLAU U, Molgaard P, Parsons AANA, Svoboda J, Virginia RARRA,
778 MØLGAARD P, Parsons AANA, J. SVOBODA, Virginia RARRA, Molgaard P, Parsons AANA,

Svoboda J, Virginia RARRA. 1997. Open-top designs for manipulating field temperature in high-latitude ecosystems. Global Change Biology 3:20–32.

McCormack ML, Dickie IA, Eissenstat DM, Fahey TJ, Fernandez CW, Guo D, Helmisaari H-S, Hobbie EA, Iversen CM, Jackson RB, Leppälammi-Kujansuu J, Norby RJ, Phillips RP, Pregitzer KS, Pritchard SG, Rewald B, Zadworny M. 2015. Redefining fine roots improves understanding of below-ground contributions to terrestrial biosphere processes. New Phytologist 207:505–18.

McKane RB, Johnson LC, Shaver GR, Nadelhoffer KJ, Rastetter EB, Fry B, Giblin AE, Kieland K, Kwiatkowski BL, Laundre JA, Murray G. 2002. Resource-based niche provide a basis for plant species diversity and dominance in arctic tundra. Nature 415:68-71.

McKendrick JD, Ott VJ, Mitchell GA. 1978. Effects of Nitrogen and Phosphorus Fertilization on Carbohydrate and Nutrient Levels in Dupontia fisheri and Arctagrostis latifolia. In: Tieszen LL, editor. Vegetation and Production Ecology of an Alaskan Arctic Tundra. Ecological Studies. New York, NY: Springer. pp 509–37. https://doi.org/10.1007/978-1-4612-6307-4_22. Last accessed 12/03/2021

McLaren JR, Darrouzet-Nardi A, Weintraub MN, Gough L. 2017. Seasonal patterns of soil nitrogen availability in moist acidic tundra. Arctic Science. https://cdnsciencepub.com/doi/abs/10.1139/as-2017-0014. Last accessed 13/04/2021

McMurtrie RE, Näsholm T. 2018. Quantifying the contribution of mass flow to nitrogen acquisition by an individual plant root. New Phytologist 218:119–30.

McRoy P, Alexander V. 1975. Nitrogen kinetics in aquatic plants in Arctic Alaska. Aquatic Botany 1:3–10.

800 Melillo JM, Butler S, Johnson J, Mohan J, Steudler P, Lux H, Burrows E, Bowles F, Smith R, Scott L,
801 Vario C, Hill T, Burton A, Zhou Y-M, Tang J. 2011. Soil warming, carbon–nitrogen interactions,
802 and forest carbon budgets. Proceedings of the National Academy of Sciences 108:9508–12.

803 Nadelhoffer KJ, Johnson L, Laundre J, Giblin AE, Shaver GR. 2002. Fine root production and nutrient
804 content in wet and moist arctic tundras as influenced by chronic fertilization. Plant and Soil
805 242:107–13.

806 Natali SM, Schuur EAG, Rubin RL. 2012. Increased plant productivity in Alaskan tundra as a result of
807 experimental warming of soil and permafrost. Journal of Ecology 100:488–98.

808 Norby RJ, Sloan VL, Iversen CM, Childs J. 2018. Controls on Fine-Scale Spatial and Temporal
809 Variability of Plant-Available Inorganic Nitrogen in a Polygonal Tundra Landscape. Ecosystems.
810 http://link.springer.com/10.1007/s10021-018-0285-6

811 Nordin A, Schmidt IK, Shaver GR. 2004. Nitrogen uptake by arctic soil microbes and plants in relation to
812 soil nitrogen supply. Ecology 85:955–62.

813 Overland JE, Wang M, Walsh JE, Stroeve JC. 2014. Future Arctic climate changes: Adaptation and
814 mitigation time scales. Earth's Future 2:68–74.

815 Post E, Alley RB, Christensen TR, Macias-Fauria M, Forbes BC, Gooseff MN, Iler A, Kerby JT, Laidre
816 KL, Mann ME, Olofsson J, Stroeve JC, Ulmer F, Virginia RA, Wang M. 2019. The polar regions
817 in a 2°C warmer world. Science Advances 5:eaaw9883.

818 Ramm E, Liu C, Ambus P, Butterbach-Bahl K, Hu B, Martikainen PJ, Marushchak ME, Mueller CW,
819 Rennenberg H, Schloter M, Siljanen HMP, Voigt C, Werner C, Biasi C, Dannenmann M. 2022. A
820 review of the importance of mineral nitrogen cycling in the plant-soil-microbe system of
821 permafrost-affected soils—changing the paradigm. Environ Res Lett 17:013004.

822 Rantanen M, Karpechko AY, Lipponen A, Nordling K, Hyvärinen O, Ruosteenoja K, Vihma T, Laaksonen
823 A. 2022. The Arctic has warmed nearly four times faster than the globe since 1979. Commun
824 Earth Environ 3:1–10.

825 Rastetter EB, Shaver GR. 1992. A Model of Multiple-Element Limitation for Acclimating Vegetation.
826 Ecology 73:1157–74.

827 Raynolds MK, Walker DA, Maier HA. 2005. Plant community-level mapping of arctic Alaska based on
828 the Circumpolar Arctic Vegetation Map. phyto 35:821–48.

829 Rodenhizer H, Natali SM, Mauritz M, Taylor MA, Celis G, Kadej S, Kelley AK, Lathrop ER, Ledman J,
830 Pegoraro EF, Salmon VG, Schädel C, See C, Webb EE, Schuur EAG. 2023. Abrupt permafrost
831 thaw drives spatially heterogeneous soil moisture and carbon dioxide fluxes in upland tundra.
832 Global Change Biology n/a. https://onlinelibrary.wiley.com/doi/abs/10.1111/gcb.16936. Last
833 accessed 11/09/2023

834 Rogers A, Gibon Y. 2009. Enzyme Kinetics: Theory and Practice. In: Schwender J, editor. Plant
835 Metabolic Networks. New York, NY: Springer. pp 71–103.
836 https://doi.org/10.1007/978-0-387-78745-9_4. Last accessed 14/09/2022

837 Rustad LE, Campbell JL, Marion GM, Norby RJ, Mitchell MJ, Hartley AE, Cornelissen JHC, Gurevitch
838 J. 2001. A meta-analysis of the response of soil respiration, net nitrogen mineralization, and
839 aboveground plant growth to experimental ecosystem warming. Oecologia 126:543–62.

840 Schimel JP, Bennet J, Bennett JB. 2004. Nitrogen mineralization: Challenges of a changing paradigm.
841 Ecology 85:591–602.

842 Screen JA, Deser C, Sun L. 2015. Projected changes in regional climate extremes arising from Arctic sea
843 ice loss. Environ Res Lett 10:084006.

844 Shaver GR, Chapin FS. 1980. Response to fertilization by various plant growth forms in an Alaskan
845 tundra: nutrient accumulation and growth. Ecology 61:662–75.

846 Shaver GR, Chapin FS, Gartner BL, Shaver AGR, Iii FC, Gartner BL, Journal S, Mar N, Gartnert BL,
847 Shaver GR, Chapin FS, Gartner BL. 1986. Factors limiting seasonal growth and peak biomass
848 accumulation in Eriophorum Vaginatum in Alaskan tussock tundra. Journal of Ecology
849 74:257–78.

850 Sistla SA, Moore JC, Simpson RT, Gough L, Shaver GR, Schimel JP. 2013. Long-term warming
851 restructures Arctic tundra without changing net soil carbon storage. Nature 497:615–8.

852 Sullivan PF, Welker JM. 2005. Warming chambers stimulate early season growth of an arctic sedge:
853 results of a minirhizotron field study. Oecologia 142:616–26.

854 Treat CC, Wollheim WM, Varner RK, Bowden WB. 2016. Longer thaw seasons increase nitrogen
855 availability for leaching during fall in tundra soils. Environ Res Lett 11:064013.

856 Ulrich A, Gersper PL. 1978. Plant Nutrient Limitations of Tundra Plant Growth. In: Tieszen LL, editor.
857 Vegetation and Production Ecology of an Alaskan Arctic Tundra. New York, NY: Springer. pp
858 457–81. https://doi.org/10.1007/978-1-4612-6307-4_20. Last accessed 15/03/2024

859 Van Wijk MT, Clemmensen KE, Shaver GR, Williams M, Callaghan TV, Chapin FS, Cornelissen
860 JHCHC, Gough L, Hobbie SE, Jonasson S, Lee JA, Michelsen A, Press MC, Richardson SJ,
861 Rueth H, Chapin III FS, Cornelissen JHCHC, Gough L, Hobbie SE, Jonasson S, Lees J,
862 Michelsen A, Press MC, Richardson SJ, Rueth H. 2003. Long-term ecosystem level experiments
863 at Toolik Lake, Alaska, and at Abisko, Northern Sweden: generalizations and differences in
864 ecosystem and plant type responses to global change. Global Change Biology 131:105–23.

865 Walker DA, Raynolds MK, Daniëls FJA, Einarsson E, Elvebakk A, Gould WA, Katenin AE, Kholod SS,
866 Markon CJ, Melnikov ES, Moskalenko NG, Talbot SS, Yurtsev BA†, The other members of the
867 CAVM Team. 2005. The Circumpolar Arctic vegetation map. Journal of Vegetation Science
868 16:267–82.

869 Wang J, Defrenne C, McCormack ML, Yang L, Tian D, Luo Y, Hou E, Yan T, Li Z, Bu W, Chen Y, Niu S.
870 2021. Fine-root functional trait responses to experimental warming: a global meta-analysis. New
871 Phytologist 230:1856–67.

872 Welker JM, Fahnestock JT, Sullivan PF, Chimner RA. 2005. Leaf mineral nutrition of Arctic plants in
873 response to warming and deeper snow in northern Alaska. Oikos 109:167–77.

874 Zhu Q, Iversen CM, Riley WJ, Slette IJ, Vander Stel HM. 2016. Root traits explain observed tundra
875 vegetation nitrogen uptake patterns: Implications for trait-based land models. Journal of
876 Geophysical Research: Biogeosciences 121.

877 Zhu Q, Riley WJ, Tang J. 2017. A new theory of plant–microbe nutrient competition resolves
878 inconsistencies between observations and model predictions. Ecological Applications 27:875–86.

879

Figure Captions

Figure 1. The impact of manipulative warming on daily soil and air temperature during the growing season. Air temperature was measured in n = 5 ZPW chambers and at one centrally located ambient weather station. Soil temperature at 10 cm depth in the soil profile was measured at n = 4 ZPW plots and n = 4 ambient sensor arrays though only 2-3 paired datasets were available through 11 July 2022 (DOY 192). Average values for growing season and each month were compared to zero, and statistical significance is denoted as follows: • for $p < 0.10$, * for $p < 0.05$, ** for $p < 0.01$. Error bars and ± represent standard error and the grey vertical bars represent the period when the $^{15}N\text{-}NH_4^+$ label was applied.

Figure 2. Impact of short-term warming on soil-extractable C and nutrient pools. Each point represents the average extractable C, N, or P pool for a given depth interval across plots (n = 5 plots per treatment, two cores averaged per plot). Error bars represent standard error. Linear models were fit with discrete parameters for warming, depth, and the interaction between warming and depth. Statistically significant model parameters are denoted as follows: • for $p < 0.10$, * for $p < 0.05$, ** for $p < 0.01$.

Figure 3. Impact of warming on resin-bound N and P following a full growing season of deployment (n = 5 plots per treatment, four resins averaged per plot). Statistically significant model parameters denoted as follows: • for $p < 0.10$, * for $p < 0.05$, ** for $p < 0.01$. TIN represents total inorganic N (NH_4^+ plus NO_3^-). Error bars represent standard error.

Figure 4. Short-term warming did not impact whole-plant NH_4^+ uptake but was associated with increased allocation of N across tissue pools. Statistically significant model parameters denoted as follows: • for $p <$ 0.10, * for $p < 0.05$, ** for $p < 0.01$.

Figure 5. Short-term warming had moderate effects on *A. latifolia* fine-root length density and biomass but did not impact morphology (SRL) or nutrient content (C:N). Statistically significant model parameters denoted as follows: • for $p < 0.10$, * for $p < 0.05$, ** for $p < 0.01$. Error bars represent standard error. (n = 5 plots per treatment, four cores averaged per plot).

Figure 6. Relationship between NH_4^+ uptake by *A. latifolia* and NH_4^+ availability in the soil. In panel a, this relationship is shown with a traditional Michaelis-Menton model fit to NH_4^+ uptake per gram root and NH_4^+ availability expressed as μM in the soil solution. In panel b, this relationship is fit with a logistic model and values are expressed as NH_4^+ uptake per cm root length and extractable NH_4^+ per cm^3 soil. Models were fit through data from both ambient and warming plots and grey shaded areas denote the 95% confidence interval for each model fit based on bootstrapping of model parameters. Values in parenthesis indicate upper and lower limits of 95% confidence intervals for parameters. Statistically significant model parameters denoted as follows: • for $p < 0.10$, * for $p < 0.05$, ** for $p < 0.01$. Analysis conducted on n = 20 harvest label locations (2 replicates labels × 5 plots × 2 treatments).

Figures

Figure 1.

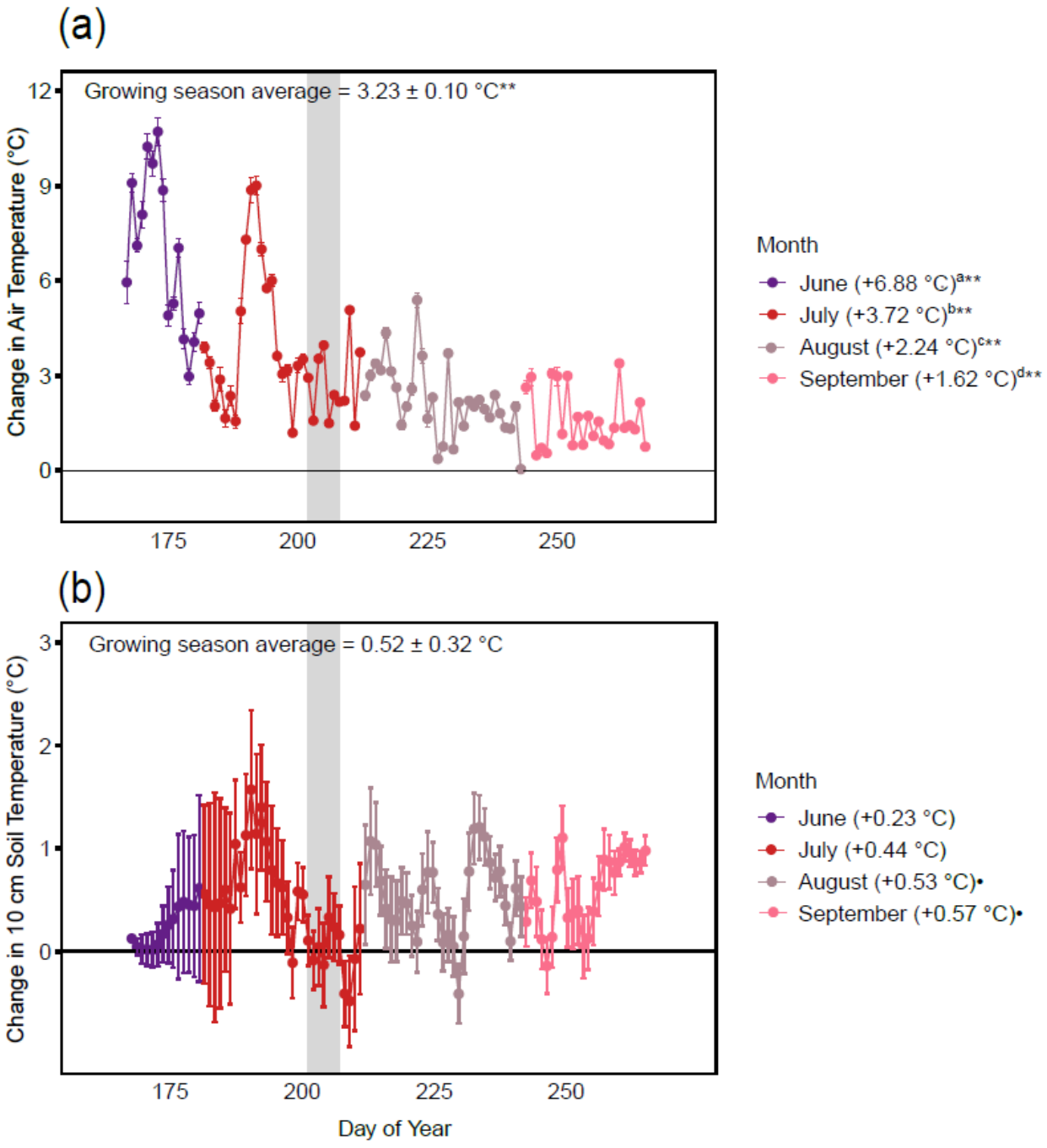

924 Figure 2.

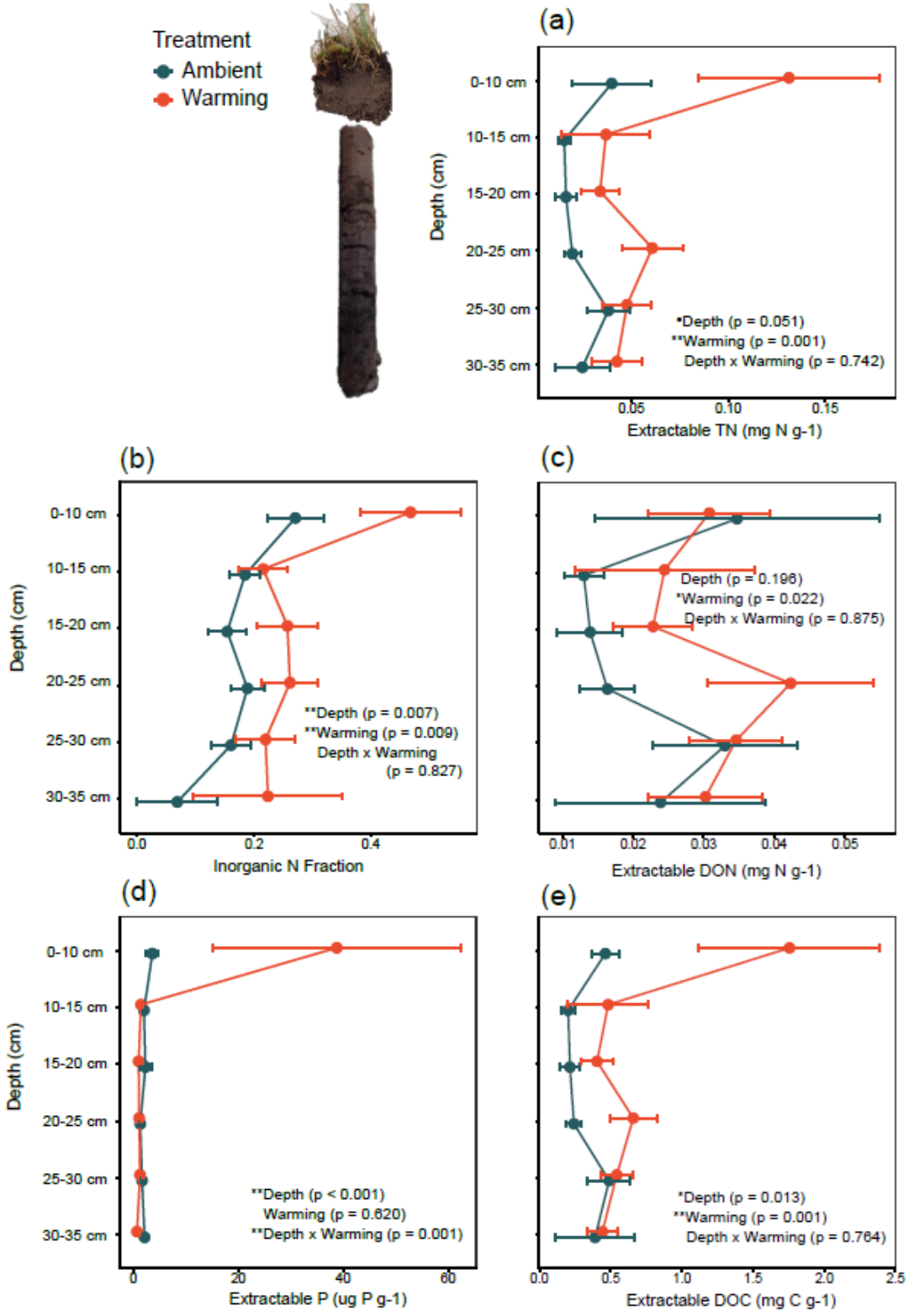

925

926

927 Figure 3.
928

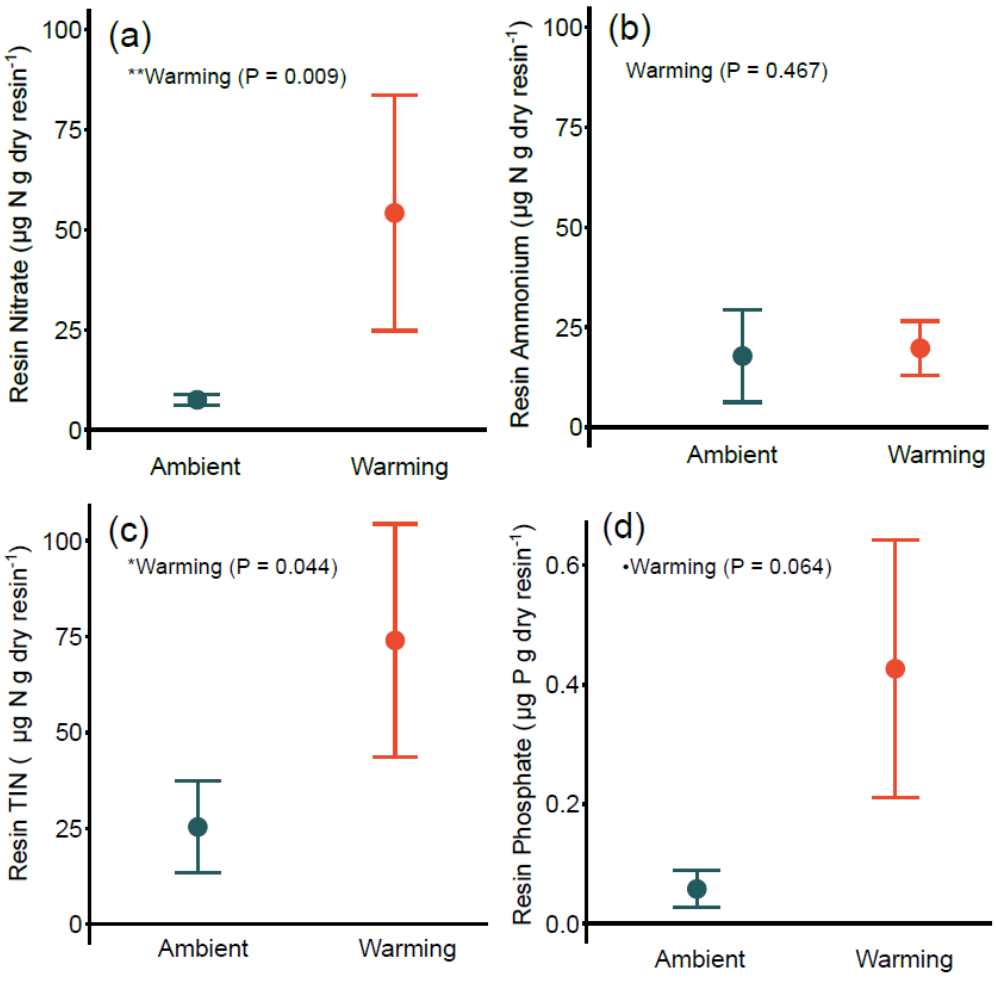

929

930 Figure 4.

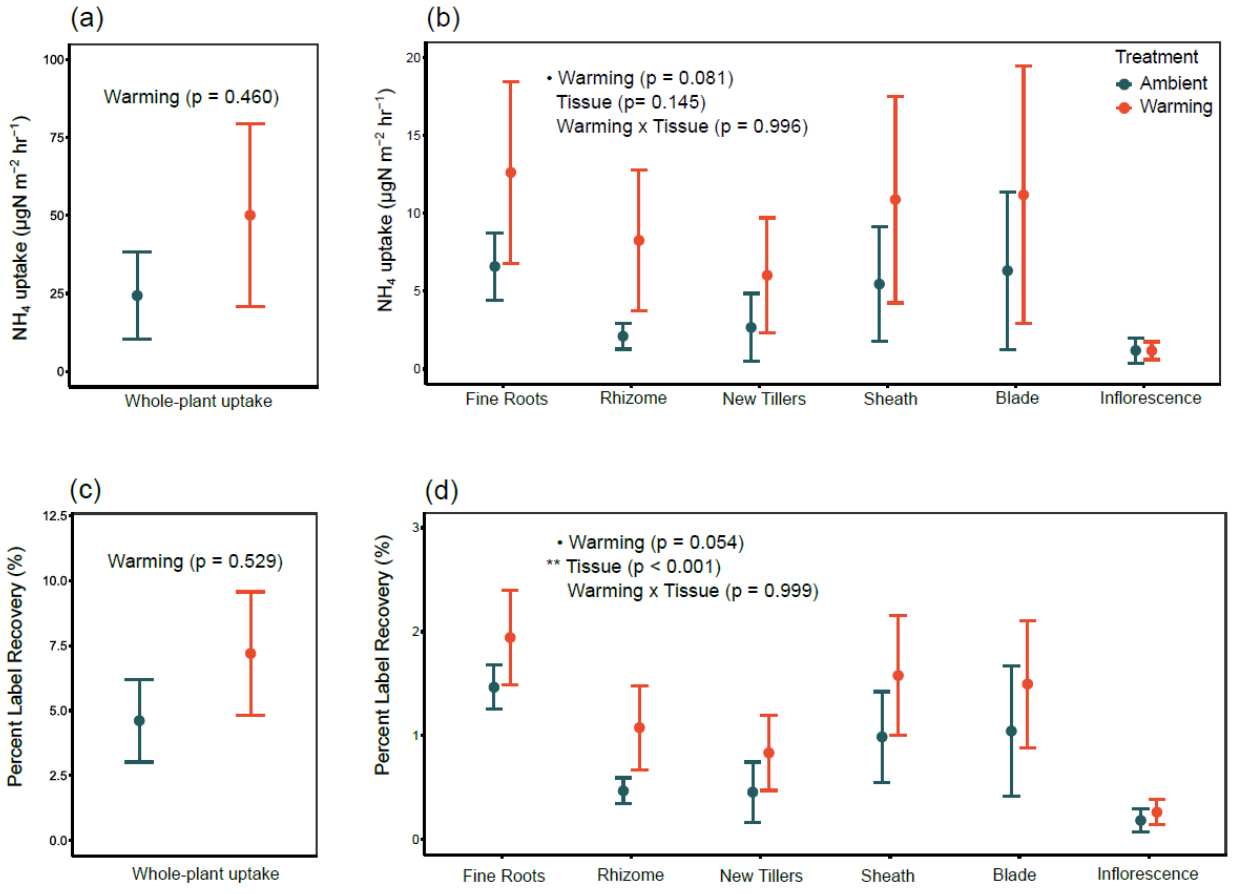

931

932 Figure 5.

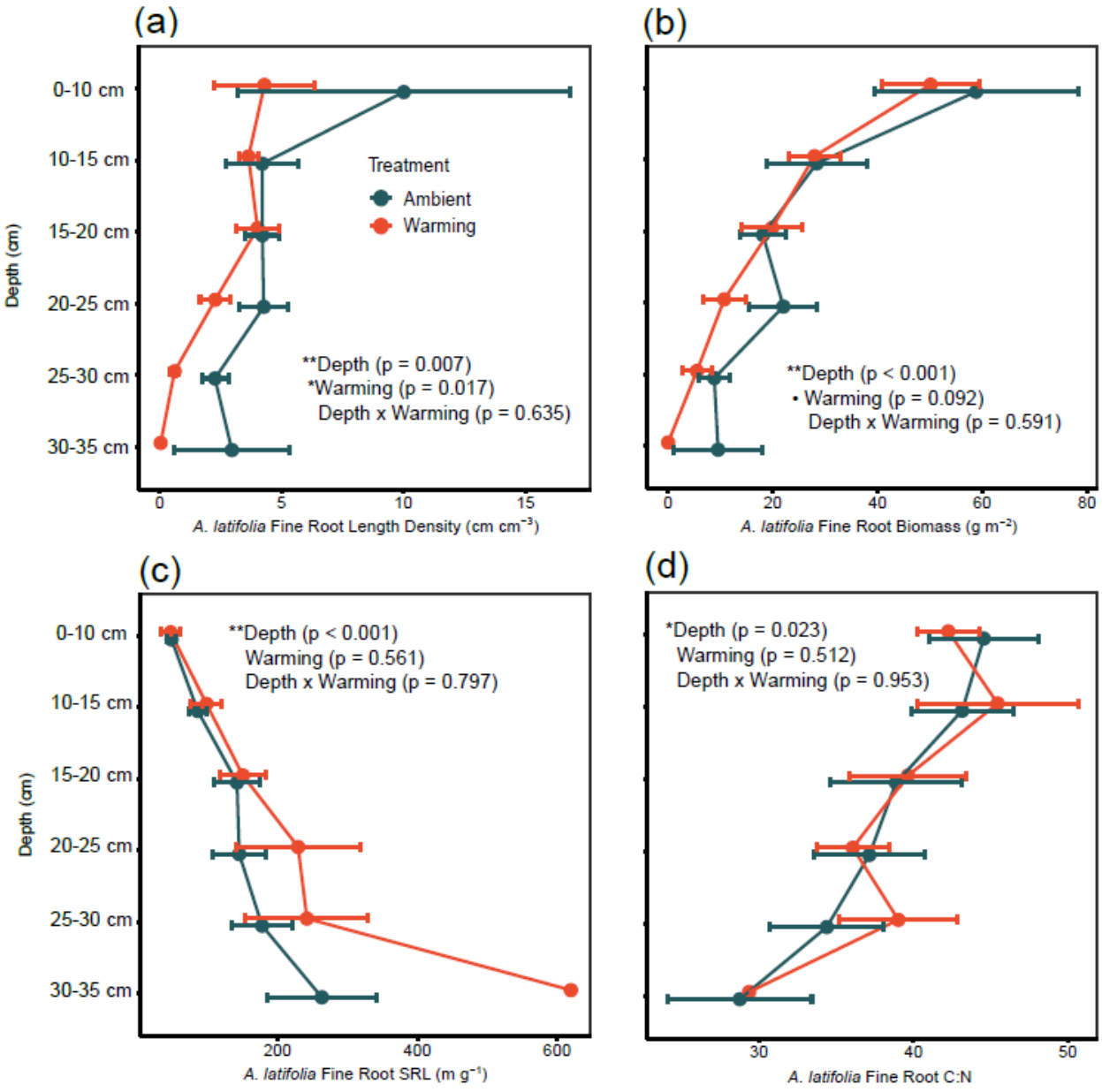

933

934

935 Figure 6.
936

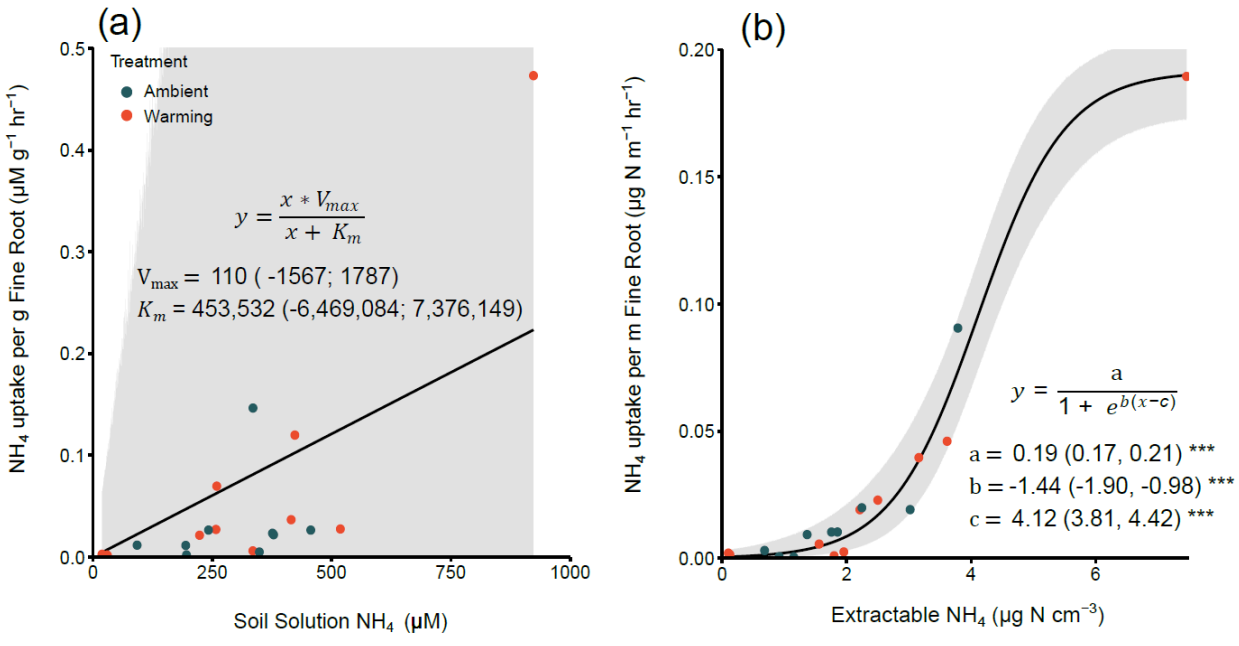

937

Table Captions

Table 1. Pools of C and N in *Arctagrostis latifolia* biomass. For all samples, data from harvests were averaged at the plot level prior to taking treatment averages (n = 5 per treatment). Means are given ± standard error. Statistically significant differences between ambient and zero power warming treatment from pool-specific t-tests are indicated with bold type and symbols (• for $p < 0.10$, * for $p < 0.05$, ** for $p < 0.01$). Statistically significant differences across tissue pools and treatments are indicated with letter superscripts based on two-way ANOVA followed by HSD Tukey test (alpha = 0.05).

Table 2. Specific Leaf Area, Leaf Area Index, and height of *Arctagrostis latifolia*. Means are given ± standard error. Statistically significant model parameters denoted with asterisks (• for $p < 0.10$, * for $p < 0.05$, ** for $p < 0.01$).

Tables

Table 1.

	Carbon pools (g C m^{-2})		Nitrogen pools (g N m^{-2})		C:N	
	Ambient	**Warming**	**Ambient**	**Warming**	**Ambient**	**Warming**
Fine Roots	63.09 ± 15.81^{a}	50.49 ± 7.06^{ab}	1.44 ± 0.28^{a}	1.24 ± 0.12^{ab}	42.07 ± 4.08^{a}	41.07 ± 2.66^{a}
Rhizomes	34.63 ± 9.95^{abc}	37.63 ± 9.15^{ab}	1.1 ± 0.29^{abc}	1.23 ± 0.29^{ab}	31.17 ± 1.99^{ab}	33.91 ± 2.53^{ab}
New Tillers	4.08 ± 1.48^{d}	4.67 ± 1.33^{d}	0.31 ± 0.10^{c}	0.31 ± 0.08^{c}	**12.71 ± 1.11^{e} ·**	**15.07 ± 0.63^{de} ·**
Sheaths	23.27 ± 4.42^{abcd}	31.47 ± 6.48^{abc}	1.11 ± 0.16^{abc}	1.24 ± 0.17^{ab}	20.63 ± 1.73^{cd}	25.27 ± 2.60^{bc}
Blades	24.16 ± 5.35^{abcd}	21.91 ± 2.35^{bcd}	1.87 ± 0.41^{a}	1.72 ± 0.19^{a}	13.04 ± 0.40^{e}	13.03 ± 0.37^{e}
Inflorescences	4.24 ± 1.68^{d}	8.4 ± 3.14^{cd}	0.31 ± 0.11^{c}	0.45 ± 0.15^{bc}	**13.24 ± 0.35^{e} ***	**16.40 ± 1.04^{de} ***
Aboveground	55.75 ± 11.12	66.45 ± 12.43	3.60 ± 0.65	3.71 ± 0.53	**15.28 ± 0.73 ·**	**17.71 ± 0.93 ·**
Belowground	97.72 ± 25.61	88.13 ± 14.18	2.54 ± 0.57	2.47 ± 0.37	37.12 ± 2.79	37.68 ± 2.41
Total	153.47 ± 29.65	154.58 ± 21.15	6.14 ± 0.96	6.19 ± 0.73	24.94 ± 1.64	25.58 ± 1.23
Above:Below	0.71 ± 0.16	0.86 ± 0.15	1.6 ± 0.29	1.74 ± 0.25		

Table 2.

	Ambient	**Warming**
Specific Leaf Area (SLA, m^2 per g)	14.54 ± 0.77	15.51 ± 0.77
Leaf Area Index (LAI)	0.79 ± 0.22	0.71 ± 0.09
Maximum Height (cm)	**16.40 ± 1.02***	**22.87 ± 2.46***